V. 4. 3D Imaging of Human Cells by Using PIXE-μ-CT

Kawamura Y.[1], Ishii K.[1], Matsuytama S.[1], Nakhostin M.[1], Fujiwara M.[1], Watanabe M.[1], Okura S.[1], Hamada N.[1], Tsuboi S.[1], Yamazaki K.[1], Hashimoto Y.[1], Fujikawa M.[1], Catella G.[1], Hatori Y.[1], Fujiki K.[1], Yamazaki H.[2], Ortega R.[3], Deves G.[3], and Carmona A.[3]

[1]*Department of Quantum Science and Energy Engineering, Tohoku University*
[2]*Cyclotron Radioisotope Center, Tohoku University*
[3]*CNAB, CNRS Universite Bordeaux 1*

Introduction

Numerous studies have shown that short-term exposure to particulate matter (PM) can adversely affect human health. For chromium compounds, the main route of exposure is via the respiratory tract by inhalation of dusts, fumes and mists. Human tissues and fluids normally contain low levels of chromium as essential element, but chromium abundance in lung tissues is increased as a result of environmental or occupational exposures and is highly carcinogenic. Some studies were carried out to know the interaction between these particles and human body at a cellular level by using the micro-PIXE/RBS and synchrotron X-ray fluorescence microprobe[1-3]. While the mechanism was suggested in these studies, distribution of chromium particles in the cell is still uncertain because 2D imaging only gives a projection image of the distribution. The 3D distribution of the chromium particles in the cell will give us crucial information on the suggested intracellular interaction mechanism between the particles and human cells. Only few imaging techniques exist that allow *in-situ* quantification and distribution of chromium particles in cell[4]. We are developing a 3D PIXE-μ-CT to observe the interior of small samples with a spatial resolution of less than 10 μm[5-10]. The 3D PIXE-μ-CT has a capability to measure intercellular distribution of Cr particles and is one of the most powerful tools. However, our system has to be optimized to observe the small structures inside a single cell. In this study, we report the 3D μ-CT for intercellular imaging and obtained the intracellular distribution of chromium compound ($PbCrO_4$).

Improvement of 3D μ-CT

The PIXE-μ-CT consists of an accelerator, a proton microbeam system, and a target chamber system equipped with X-ray CCD camera[5-10]. In the PIXE-μ-CT configuration, the X-ray point source and the X-ray CCD are fixed while the sample is placed between them is rotated. In this system, 2D X-ray projection data are obtained for each rotation angle of the sample and therefore a 3D image can be reconstructed. X-ray generated with this system consists mainly of characteristic X-ray of target element which is quasi-monoenergetic[11]. These properties allow getting a high-contrast imaging of cells which makes the system suitable for this biological samples analysis as exemplified in insect studies[7-10].

For intracellular imaging, higher contrast and higher spatial resolution are required in the PIXE-μ-CT system. For this purpose, we have taken the following steps. First, to improve the contrast of CT images, we selected an appropriate X-ray producing target. Second, to obtain higher spatial resolution projection image, we investigated cone beam magnification geometry and also, the precision of sample rotation was improved.

Improvement of the Contrast

In order to visualize microscopic biological sample like cells using PIXE-μ-CT, high contrast X-ray transmission data is needed. Considering the X-ray transmission of the cell and detection efficiency of the CCD camera, X-ray energy of 3 to 5 keV is appropriate for this study. This can be achieved by employing scandium as target.

Improvement of the CT image resolution

In PIXE-μ-CT system, the projection data of the sample is taken by using cone beam magnification geometry. Therefore, the spatial resolution of the CT image is affected by the following two parameters, effective pixel size and blur of the projection data. These parameters are strongly affected by the finite focal spot size and the magnification factor. For the ideal X-ray source that can be considered to be point source, we can obtain higher resolution images as the magnification increases. As shown in the following equation, the image resolution is improved by increasing the magnification:

$$r_{CCD} = \frac{2 \times pixelsize}{m} \qquad (1)$$

where r_{CCD} is the effective pixel size in the object plane and *pixelsize* is the CCD pixel size

(=8 μm) in the image plane and *m* is the magnification. The magnification was restricted to around 4 to 5 in previous studies[7-10] because of finite sample size and the finite size of CCD. In this study, cell sample is smaller than those used in the previous studies, thus we can obtain better resolution by increasing magnification. However, actual projection data is affected by blurring that surrounds an object. This causes the edge to be reproduced with an optical density gradient by the imaging system. The extent of the blurring is related to the focus size and magnification:

$$Blur = (m-1) \times f \tag{2}$$

where f is the focal spot size. The shape of sample is estimated by the image data projected to the detector screen. Therefore, the spatial resolution distorted by the finite focal spot is as follows:

$$r_{blur} = Blur / m = \frac{(m-1) \times f}{m} \tag{3}$$

Figure 1 shows the relationship between the detector sampling pitch and the image blurring with respect to the magnification. In general, at lower magnification the detector sampling pitch is a limiting factor of the resolution; at higher magnification the blurring caused by focal spot becomes critical for the resolution. In addition, there is an optimal magnification for each focal spot size. In previous study, we obtained the spatial resolution of 4 μm at a magnification of nine with a beam spot size of 1.5×1.5 μm. However, the resolution was worse than the calculated value. This was due to the fact that, in that calculation, the focal spot size was not considered. Thus the calculated resolution was less than the actual one. The present estimation is quite consistent with the experimental results. It shows that resolution will improve as an increase of the magnification and will saturate down to the beam spot size.

Figure 2 shows the CT image of a polyimide tube (inner diameter of 80 μm, wall thickness of 10 μm) and the intensity profile of CT-value, acquired in a condition corresponding to a proton beam energy of 3 MeV, proton beam spot size of 1.1×1.1 μm^2 and magnification of 12.4. The measured profile was fitted by symmetric double Gaussian convolution to obtain the spatial resolution of the system. The resolution of the system was evaluated to be around 3.4 μm, which is consistent with the estimation.

Sample preparation

In this study, we analyzed human epithelial cells exposed *in vitro* to $PbCrO_4$.

Fixation of the cells on the rotating shaft is one of the biggest problems in this study. A micro polycarbonate tube (MicroLumen 030-I; 80 μm inside diameter and 10 μm thickness) was used to fix the cells. The tube is the smallest and thinnest commercially available. Since size of the cell is in the order of 10 to 20 μm, tube thickness is almost same order and not deteriorates the contrast. The cells were fixed in the inner wall of the tube. Then the end of the tube is inserted into the injection needle, and then fixed to rotation shaft. We adopted cryogenic methods to fix the cell in the tube, since they consist of immobilizing the intracellular components by cryofixation and later extraction of the water by freeze drying process. The protocol is almost the same as that for SXRF and PIXE analysis[3)], except for encapsulate process. Capillary action was used to insert the cell into the tube. After that, the tube was sealed with formvar and cryofixed at -164°C into isopentane chilled with liquid nitrogen. Then the sample was freeze dried at -35°C for 1 week after removing the seal.

Result and Discussion

Human epithelial cells exposed *in vitro* to 1 μm/cm^2 $PbCrO_4$ for 24 h were analyzed by using the PIXE-μ-CT. Measurement was carried out with 3 MeV proton beam, beam currents of ca. 400 pA, beam spot size of 1.1×1.1 μm^2. Geometric magnification was 12.4. X-ray target is Sc and target was set at 30 degrees with respect to the beam direction. Figure 3 shows the 2D cross sectional view of cell and line profile of pixel value. The image was reconstructed on the basis of image data in the vertical plane by using an iteration method (Maximum Likelihood-Expectation Maximization method). The pixel value of micro tube and cell is different showing a good contrast. While cell density will be similar to that of the tube, higher absorption of X-ray by $PbCrO_4$ particles increased the absorption in the cell. Figure 4 shows the 3D imaging of human epithelial cells from the different angles. The size of the cells is around 20 μm and consistent with microscopic images. The region marked with arrow in the right figure, could be a cell which did not absorb, or absorbed less $PbCrO_4$ than the others. The pixel value is almost same as that of the tube. The region which shows strong absorption means the $PbCrO_4$ particles. Two kind of distribution are seen; one is distributed over the cell area, the other is concentrated in small structures within the cell.

Conclusion

The CT images of the human epithelial cells were obtained by using the PIXE-μ-CT. To observe the microstructure of sample, we improved the existing system. For the image contrast, Sc was selected as an X-ray target and obtained a good contrast of cell projections. For the image resolution, the rotating stage was improved and the magnification geometry was optimized. Thus intracellular distributions of the lead chromate particles could be observed. The PIXE-μ-CT will give us the crucial information on the interaction between the particulate matter and human cells indicating that lead chromate is internalized and that is distribution is both diffused within the all cell volume, and located in small structures inside cells. This result is consistent with the suggested mechanism of action of lead chromate[3] which can be partially soluble in cells, explaining the diffuse distribution, and partially insoluble, explaining the high local concentration within intracellular structures.

Acknowledgements

This study was partly funded by a Grants-in-Aid for Scientific Research, (S) No. 13852017 from the Ministry of Education, Culture, Sports, Science and Technology, Japan. This study was also supported by JSPS and MHEST under the Japan-France Research Cooperative Program (Partenariat Hubert Curien - SAKURA Project).

The authors would like to acknowledge the assistance of Fujisawa M. for maintenance and operation of the Dynamitron accelerator. The authors would like to thank Mr. Nagaya T. and Komatsu K., for their assistance in constructing the system.

References

1) Ortega, R., Devès G., Fayard B., Salomé M., Susini J., Nucl. Instru. Meth. **B210** (2003) 325.
2) Ortega, R., Fayard B., Salomé M., Devès G., Susini J., J. de Physique IV, **104** (2003) 289.
3) Ortega, R., Fayard B., Salomé M., Devès, G.Susini J., accepted in Chemical Research in Toxicology (2005).
4) Ortega R., Sarkar Ed. B., Marcel Dekker Inc., New York (2002) pp.35-68
5) Ishii K., Matsuyama S., Yamazaki H., Watanabe Y., Yamaguchi T., Momose G., Amartaivan Ts., Suzuki A., Kikuchi Y. and Galster W., I. J. PIXE **15** (2005) 111.
6) Yamaguchi T., Ishii K., Yamazaki H., Matsuyama S., Watanabe Y., Abe S., Inomata M., Ishizaki A., Oyama R., Kawamura Y., , I. J. PIXE **15** (2005)195.
7) Ishii K., Matsuyama S., Yamazaki H., Watanabe Y., Kawamura Y., Yamaguchi T., Momose G., Kikuchi Y., Terakawa A., Galster W., Nucl. Instr. Meth., **B249** (2006) 726.
8) Ishii K., Matsuyama S., Watanabe Y., Kawamura Y., Yamaguchi T., Oyama R., Momose G., Ishizaki A., Yamazaki H., Kikuchi Y.. Nucl.Instr. and Meth. **A571** (2007) 64.
9) Kawamura Y., Ishii K., Yamazaki H., Matsuyama S., Kikuchi Y., Yamaguchi T., Watanabe Y., Oyama R., Momose G., Ishizaki A., Tsuboi S., Yamanaka K. and Watanabe M., I. J. PIXE **17** (2007) 41.
10) Ohkura S., Ishii K., Matsuyama S., Yamazaki H., Terakawa A., Kikuchi Y., Fujiwara M., Kawamura Y., Tsuboi S., Yamanaka K., Watanabe M. and Fujikawa M., I. J. PIXE **18** (2008) 167.

11) Ishii K., Morita S., I. J. PIXE **1** (1990) 1.

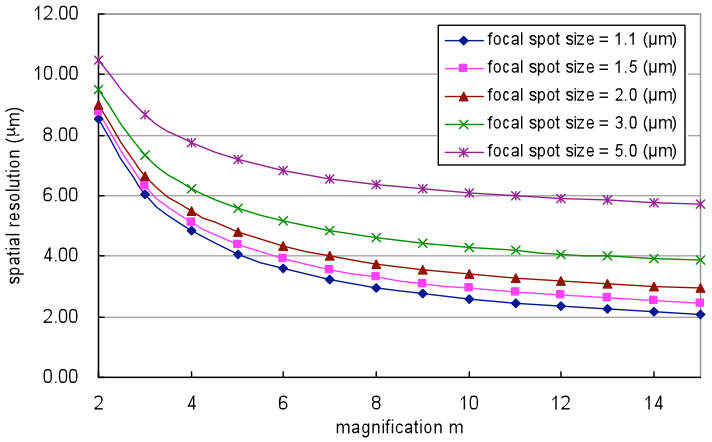

Figure 1. Relationship between spatial resolution and magnification.

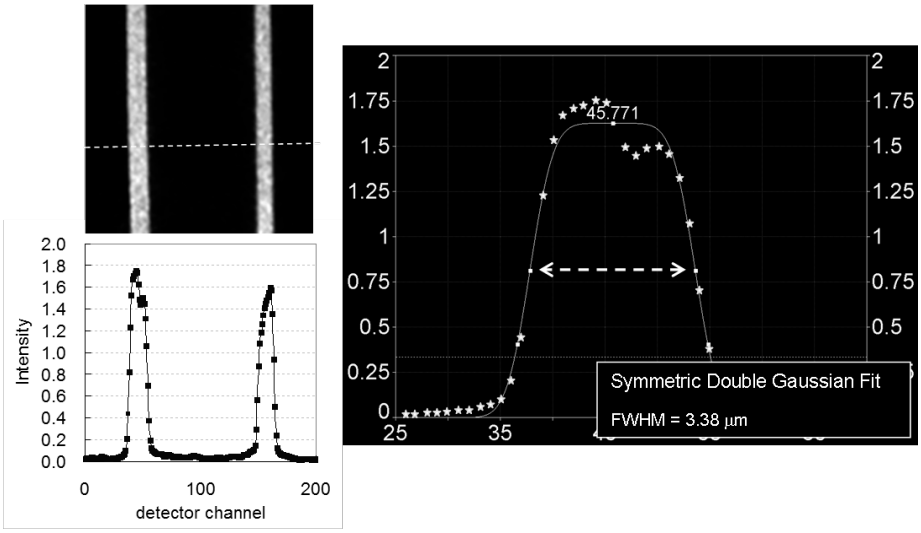

Figure 2. CT image of capillary tube and the profile of the intensity of CT-value.

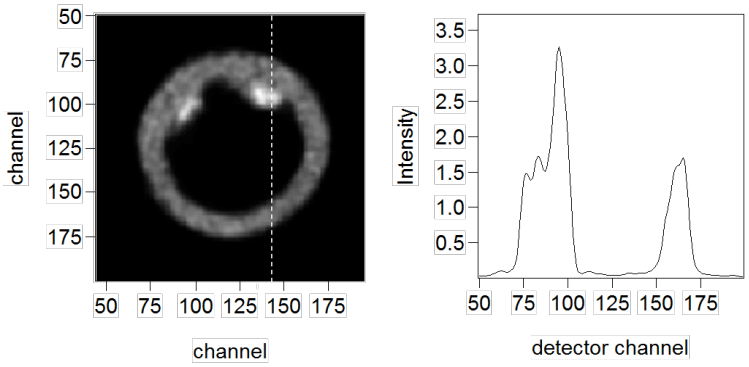

Figue 3. Cross sectional view of cell and Line profile.

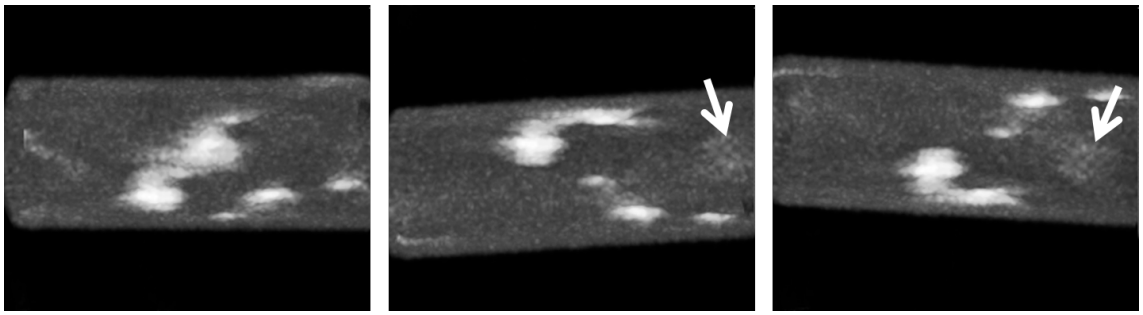

Figure 4. Maximum Intensity Projection (3D imaging from different angles).